# Chapter 2. WEATHER GENERATOR

**A.D. Nicks, L.J. Lane and G.A. Gander**

## 2.1 Weather Generator and Equations

The weather generation methods used in the WEPP model are based on the generators used in the EPIC (Williams et al., 1984), and SWRRB (Williams et al., 1985) models. This selection was based on the following: 1) the existing generators had been well tested in many location across the United States (Nicks, 1985) (see Figure 2.1.1), 2) the inputs for these models had been developed for nearly 200 stations, and 3) parameter estimation software and techniques were available. The weather generation methods used in the existing models have been modified to include the additional requirements for rainfall intensity distributions. The following section describes the equations and algorithms for the various components of the WEPP weather generator, also known as CLIGEN.

Figure 2.1.1. Test locations for Weather Generator for EPIC and SWRRB models.

### 2.1.1 Precipitation Occurrence

The method used for generating the number and distribution of precipitation events is a two-state Markov chain. This method involves the calculation of two conditional probabilities: α, the probability of a wet day following a dry day, and β, the probability of a dry day following a wet day. The two-state Markov chain for the combination of conditional probabilities is

$$P(W \mid D) = \alpha \qquad [2.1.1]$$

$$P(D \mid D) = 1 - \alpha \qquad [2.1.2]$$

$$P(D \mid W) = \beta \qquad [2.1.3]$$

$$P(W \mid W) = 1 - \beta \qquad [2.1.4]$$

where $P(W \mid D)$, $P(D \mid D)$, $P(D \mid W)$, and $P(W \mid W)$ are the probabilities of a wet given a dry, dry given a dry, dry given a wet, and a wet given a previous wet day, respectively. Twelve monthly values of these probabilities are calculated and used to provide a transition from one season to another. Random sampling of the monthly distributions is then used to determine the occurrence of a wet or dry day.

**2.1.2 Precipitation Amount**

A skewed normal distribution is used to represent the daily precipitation amounts for each month. The form of this equation is

$$x = \frac{6}{g}\left\{ \frac{\left[ \frac{g}{2}\left( \frac{X-u}{s} \right) + 1 \right]^{1}}{3} - 1 \right\} + \frac{g}{6} \qquad [2.1.5]$$

where $x$ is the standard normal variate, $X$ is the raw variate, and $u$, $s$, and $g$, are the mean, standard deviation, and skew coefficient of the raw variate, respectively. The mean standard deviation and skew coefficient of daily amounts are calculated for each month. Then, to generate a daily amount for each wet day occurrence, a random normal deviate is drawn and the raw variate, $X$ (daily amount), is calculated using Eq. [2.1.5]. If the maximum daily temperature is below zero degrees Celsius ($0^{o}C$) any precipitation is predicted to occur as snow. If the maximum daily temperature is above zero degrees Celsius and the minimum daily temperature is below zero degrees Celsius, the precipitation may be predicted to occur as rain or as snow. Information on how the WEPP model determines snow or rainfall occurrence in such a situation is provided in Chapter 3 of this documentation.

**2.1.3 Storm Duration**

The method used to estimate the duration of generated precipitation events is that used in the SWRRB model (Arnold et al., 1990). It is assumed that the duration of storm events is exponentially related to mean monthly duration of events given by

$$D = \frac{9.210}{-2 \ln (1 - rl)} \qquad [2.1.6]$$

where $D$ is the event duration ($h$) and $rl$ is a dimensionless parameter from a gamma distribution of the half-hour monthly average precipitation amounts.

### 2.1.4 Peak Storm Intensity

The peak storm intensity is estimated by a method proposed by Arnold and Williams (1989), given as

$$r_p = -2\,P\,\ln(1 - rl) \qquad [2.1.7]$$

where $r_p$ is the peak storm intensity ($mm \cdot h^{-1}$), $P$ is the total storm amount ($mm$) and $rl$ is as described previously.

Time from the beginning of the storm to the peak intensity is estimated by calculating the annual accumulated distribution of time to peaks from the National Weather Service 15 minute recording stations data. These stations record the amount of precipitation that falls in 15 minute clock hour time intervals. The precipitation amounts are reported to the nearest 2.54 mm (0.10 in.). The time to peak of each storm is calculated from the beginning of the first precipitation interval to the mid-point of the 15 minute interval containing the peak intensity. All inter-storm periods with zero rainfall are removed from the total storm duration, resulting in an effective duration of only intervals with precipitation. Then the time to peak is assigned to one of twelve class intervals of storm duration in the range of 0.0 to 1.0 by

$$k = D_p \,/\, (0.08333\, D_e) \qquad [2.1.8]$$

where $k$ is the class interval, $D_p$ is the time to peak, and $D_e$ the effective precipitation duration. An accumulated distribution of time to peaks of all storms throughout the year is then constructed by summing the fraction of the number events in each class interval. And by

$$A_k = \frac{N_k}{N} \qquad [2.1.9]$$

where $A_k$ is the accumulated frequency for the interval $k$ = 1,2,...12, $N_k$ is the number of storms with time to peaks in the interval, and $N$ is the total number of events in the station record.

The distribution of 15 minute stations are shown in Figure 2.1.4. The time to peak distributions derived, as given above, are then distributed by interpolation procedures to the precipitation and temperature stations shown in Figure 2.1.3. Thus, a site specific time to peak can be calculated for each generated storm amount by sampling the accumulated distribution with a uniform random deviate between 0.0 and 1.0.

The rainfall depth-duration-frequency relationship produced by the weather generator is sensitive to the peak storm intensity, $r_p$, and the duration of the event, $D$. Equations [2.1.6] and [2.1.7] for the storm duration and peak storm intensity, respectively, are tentative and subject to modification as more historical precipitation data are analyzed. In addition, historical tabulations of rainfall depth-duration-frequency data for durations up to 24 hours include multiple storms in the total daily rainfall. Further research is needed to analyze the national database of hourly and breakpoint precipitation data to determine regional probability distributions for the number of storms per day, their duration, individual peak intensities, and the resulting influence on the apparent rainfall depth-duration-frequency relationships.

### 2.1.5 Air Temperature

The dependency of air temperature on a given day to the precipitation occurrence condition, is that for dry days following dry days, temperatures tend to be higher than normal and for wet days following wet days, temperatures tend to be lower. Similar results are seen for wet following dry and dry following wet days (Nicks and Harp, 1980), (Richardson, 1981). The relationships used in the WEPP climate generator are

$$T_{max} = T_{mx} + (ST_{mx})(v) \tag{2.1.10}$$

$$T_{min} = T_{mn} + (ST_{mn})(v) \tag{2.1.11}$$

where $T_{max}$ and $T_{min}$ are generated maximum and minimum temperatures, $T_{mx}$ and $T_{mn}$ are the mean daily maximum and minimum temperatures for a given month, $ST_{mx}$ and $ST_{mn}$ are the standard deviation of maximum and minimum temperature for the month and $v$ is a standard normal deviate.

### 2.1.6 Solar Radiation

The generation of daily solar radiation is performed in a similar manner as temperature using a normal distribution of daily values during a month. Daily generated solar radiation is given by

$$RA = RA_m + (U_{ra})(x) \tag{2.1.12}$$

where $RA$ is the generated daily solar radiation, $RA_m$ is mean monthly solar radiation, $U_{ra}$ is the standard deviation for daily solar radiation and $x$ is a standard normal variate. The generated solar radiation is constrained between a maximum value possible for the day of the year, $RA_{max}$, and a minimum value currently set at 5% of the maximum value. The maximum radiation possible is computed from the location of the station and the sun angle on the day to be generated. The standard deviation is estimated by

$$U_{ra} = RA_{max} - \frac{RA_m}{4} \tag{2.1.13}$$

### 2.1.7 Dew Point Temperature

Dew point temperatures are generated in the model by

$$T_{dp} = T_{dpo} + (ST_{mn})\,(v) \tag{2.1.14}$$

where $T_{dp}$ is the generated daily dew point temperature, $T_{dpo}$ is the mean monthly dew point temperature, and $v$ is a standard normal deviate.

### 2.1.8 Wind Speed and Direction

Wind speed and direction are required in the WEPP models for the calculation of snow accumulation, snow melting, and evapotranspiration. The method used to generate wind direction is based on the division of historical wind data into 16 cardinal directions by percent of time the wind is blowing from that direction. An accumulated distribution of percent of time that wind is blowing each of these directions is derived from the wind data in the same manner as the time to peak distribution was constructed. A uniform random number between 0 and 1 is drawn to sample the accumulated distribution of wind directions. After the direction is calculated, the wind speed for that direction is generated using Eq. [2.1.5] and a standard normal deviate. But in this case, the mean, standard deviation, and skew coefficients of daily wind speed are used as the parameters.

### 2.1.9 Historical Data

Daily, hourly, and 15-minute data were obtained from the National Climatic Data Center. These data were inventoried and approximately 7000 stations were found with precipitation or precipitation and temperature with 25 years or more of record lengths (Figure 2.1.2). A subset of approximately 1200 stations with both precipitation and maximum and minimum air temperature based on a grid of one degree of latitude by one degree of longitude were selected for parameterization. The distribution of these stations are shown in Figure 2.1.3. At each station, parameters for all other climate elements were also calculated. Similarly, stations were selected in Alaska, Hawaii, Puerto Rico, and the U.S. Pacific islands, resulting in a generator parameter database for each of the 50 U.S. states and territories. Figure 2.1.4 shows the distribution of 15-minute precipitation stations used to derive time to peak intensity distribution at each daily climate station. Distribution of the solar radiation and dew point data stations are shown in Figure 2.1.5 and Figure 2.1.6. Wind speed and direction stations used are shown in Figure 2.1.7.

Currently under investigation is the use of a Geographic Information System (GIS) to allow subsequent mapping of the parameter values. Linking of the climatic database developed under the WEPP with a GIS would allow the user agencies more flexibility in the parameter selection than specific site values. It may also provide a partial solution to problems that have plagued the user of climatic data in remote areas of the western mountain areas of the United States. Current studies are investigating the possible use of GIS as a method to provide interpolation between the few high altitude climatic stations.

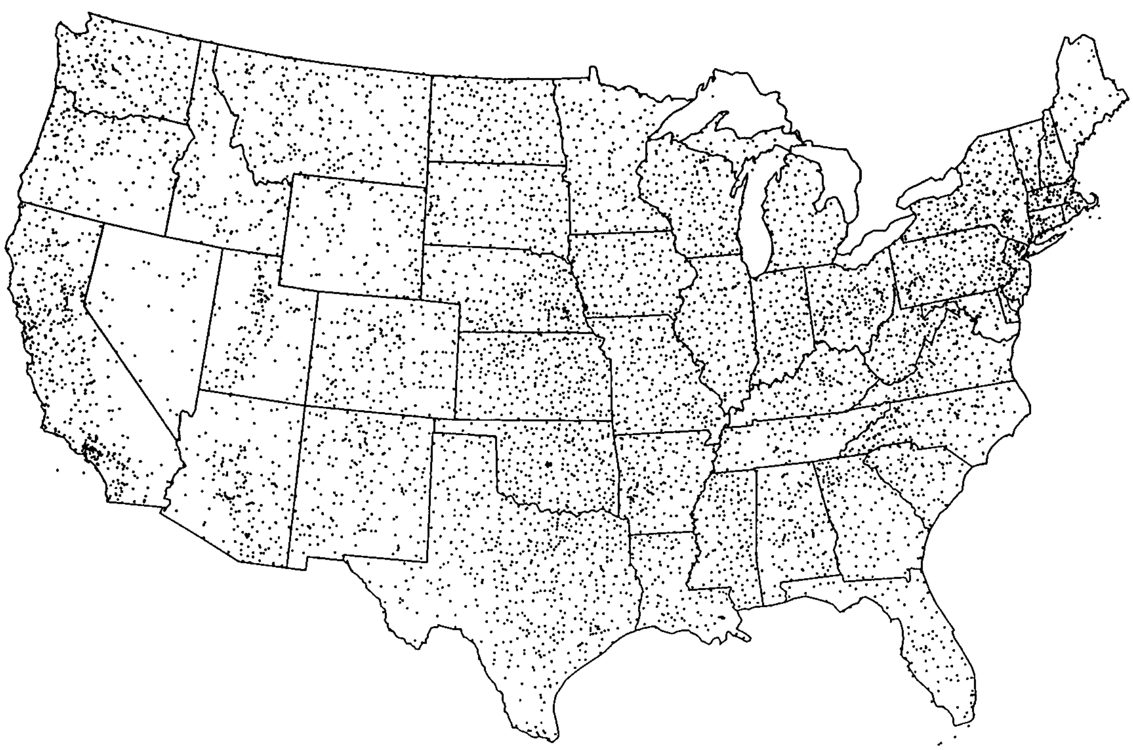

Figure 2.1.2. Weather stations from the National Climatic Data Center.

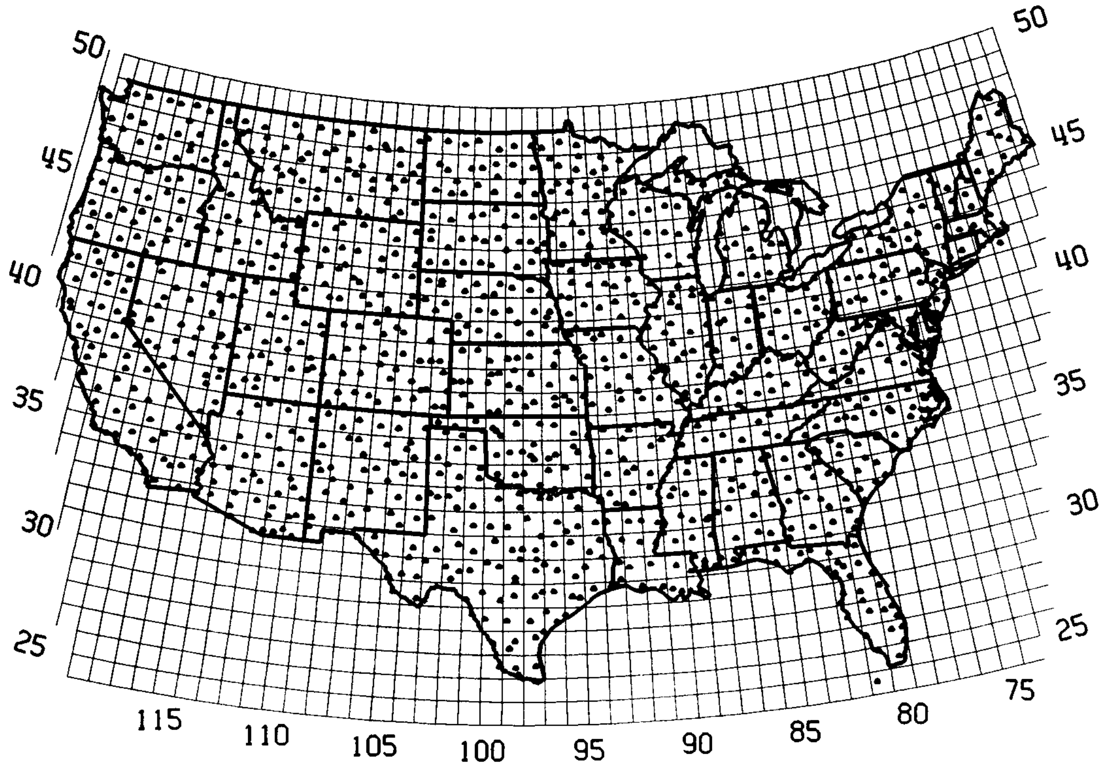


Figure 2.1.3. Subset of precipitation and air temperature stations selected for parameterization.

Figure 2.1.4. Distribution of 15-minute precipitation stations.

Figure 2.1.5. Solar radiation stations.

Figure 2.1.6. Dew point temperature stations.

Figure 2.1.7. Wind speed and direction stations.

## 2.2 Storm Disaggregation for Rainfall Intensity Patterns

To apply the Green-Ampt infiltration equation in computing infiltration and thus runoff (see Chapter 4), rainfall input data must be in the form of breakpoint data. A file in breakpoint data form contains two columns with cumulative time from the beginning of the storm in the first column and average rainfall intensity over the time interval between successive times in the second column. This form is called breakpoint because the data result from numerical differentiation of the cumulative time vs. cumulative rainfall depth curve at the changes in slope or breakpoints.

Example calculations for a hypothetical storm are summarized in Table 2.2.1. Column 1 is the cumulative time (*min*) from the start of the rainfall storm and column 2 is the cumulative rainfall depth (*mm*) at the given times. Column 3 is the rainfall intensity ($mm \cdot h^{-1}$) calculated from columns 1 and 2 as follows. From time = 0 to time = 5 min, 2.0 mm of rain fell. Therefore, the average rainfall intensity ($mm \cdot h^{-1}$) from time 0 to 5 min is computed as

$$i = \left[ \frac{2.0 - 0.0 \; mm}{5.0 - 0.0 \; min} \right] \frac{60 \; min}{h} = 24.0 \; \frac{mm}{h} \qquad [2.2.1]$$

and the average rainfall intensity from time 5 to 7 min is computed as

$$i = \left[ \frac{10.0 - 2.0 \; mm}{7.0 - 5.0 \; min} \right] \frac{60 \; min}{h} = 240.0 \; \frac{mm}{h} \qquad [2.2.2]$$

Notice that a first value of intensity is listed at time zero. This means that from time zero until the first time (5 min in this case) the average rainfall intensity was 24.0 $mm \cdot h^{-1}$. The last intensity value in column 3 of Table 2.2.1 is zero. The storm ended at time = 30 min, so rainfall intensity from 30 min on is listed as zero. A similar convention (nonzero intensity value at time zero and zero intensity value at the last time given for the storm) is used throughout the WEPP computer programs.

Table 2.2.1. Example of rainfall intensity calculations using breakpoint data.

| Time | Rainfall Depth | Rainfall Intensity | Normalized | |
|---|---|---|---|---|
| (*min*) | (*mm*) | ($mm \cdot h^{-1}$) | Time | Intensity |
| (1) | (2) | (3) | (4) | (5) |
| 0. | 0.0 | 24.0 | 0.0 | 0.60 |
| 5. | 2.0 | 240.0 | 0.167 | 6.00 |
| 7. | 10.0 | 80.0 | 0.233 | 2.00 |
| 10. | 14.0 | 18.0 | 0.333 | 0.45 |
| 20. | 17.0 | 18.0 | 0.667 | 0.45 |
| 30. | 20.0 | 0.0 | 1.000 | 0.0 |

Again, columns 1 and 3 in Table 2.2.1 would be used as input data to the infiltration calculations while columns 1 and 2 would represent typical data from a recording rain gauge. Data shown in columns 4 and 5 of Table 2.2.1 will be discussed in section 2.2.1.

Development of data such as in Table 2.2.1 for a 10- to 20-year period at a particular location to use in calculating infiltration for WEPP would be very laborious. Disaggregation of total storm data into rainfall intensity patterns with properties similar to those obtained from analysis of observed breakpoint data could save a great deal of effort. That is, given a storm amount and storm duration, approximate intensity patterns which will yield similar infiltration, runoff, and erosion can be developed. The following sections provide a brief background and describe the method used in deriving approximate rainfall intensity data from data on storm amount and duration.

Schaake et al. (1972) described a multivariate technique to generate rainfall for annual, seasonal, monthly, and daily events. The generation method involved the staged disaggregation of rainfall from annual to seasonal, seasonal to monthly, and finally monthly to daily values.

Franz (1974) developed a procedure to generate synthetic, hourly rainfall data within a storm and used empirically derived parameters to model hour to hour storm amounts with a multivariate normal distribution. An hour of zero rainfall was used to define the end of a storm period. Skees and Shenton (1974) noted that annual and monthly rainfall amounts had been successfully modeled as random variables with gamma, normal, and logarithmic normal distributions. For shorter intervals (weeks, days, hours), satisfactory distributions were more difficult to obtain.

Austin and Claborn (1974) derived a method to distribute the rainfall during storm events but assumed that no significant serial correlation existed between rainfall periods within the storm. A series of independent storm intensities were generated, then adjusted, to preserve the previously generated storm amount and duration. The procedure generated independent 4-minute intensities within the storm although analyses of observed data suggested the need for a serial correlation between 4-minute rainfall intensities.

Hershenhorn and Woolhiser (1987) reviewed previous rainfall disaggregation methods proposed by Betson et al. (1980) and Srikanthan and McMahon (1985). Both methods were described as needing very large numbers of parameter estimates, and a procedure was proposed of a more parameter-efficient approach. Hershenhorn and Woolhiser (1987) disaggregated daily rainfall into one or more individual storms and then disaggregated the individual storms into rainfall intensity patterns. The disaggregated data included starting times of the events as well as the time-intensity data within each event.

Flanagan et al. (1987) studied the influence of storm pattern (time to peak intensity and the maximum intensity) on runoff, erosion, and nutrient loss using a programmable rainfall simulator. Six rainfall patterns and three maximum intensities were used. Although the storm patterns were constant, triangular, and compound consisting of four straight line segments, all patterns could be described fairly well by a double exponential function. The double exponential function or distribution describes rainfall intensity as exponentially increasing with time until the peak intensity and then exponentially decreasing with time until the end of the storm.

The WEPP User Requirements (Foster and Lane, 1987) suggested that the maximum information required to represent a design storm consist of the following: (a) storm amount, (b) average intensity, (c) ratio of peak intensity to average intensity, and (d) time to peak intensity. Examination of appropriate functions to describe a rainfall intensity pattern given this information suggested consideration of a triangular distribution and a double exponential distribution. Because the area of a triangle is one half the product of the base (storm duration) and the height (maximum or peak intensity), the ratio of peak intensity to average intensity for a triangular distribution is fixed at exactly 2. Therefore, intensity patterns within a single storm are represented in the WEPP model with the double exponential function.

**2.2.1 Definition of Variables**

If all times during a storm are normalized by the storm duration, $D$, and all intensity values are normalized by the average intensity, $i_b$, then the result is called a normalized intensity pattern and is shown in columns 4 and 5 in Table 2.2.1. The area under the normalized time-intensity curve is 1.0 and the normalized duration is also 1.0.

Let the normalized time be $t$ and the normalized intensity be $i(t)$. The normalized time until the peak intensity, $t_p$, is calculated as the time to peak intensity over the storm duration. In the example in Table 2.2.1, the maximum rainfall intensity occurs from time = 5 to time = 7 min. Let the time to peak intensity be 6.0 min so that

$$t_p = \frac{D_p}{D} = \frac{6.0}{30.0} = 0.2 \qquad [2.2.3]$$

is the normalized time to peak intensity, $i_p$. The normalized peak intensity is calculated as the peak intensity over the average intensity. In the example in Table 2.2.1, the maximum intensity is 240 $mm \cdot h^{-1}$ and the average intensity is 40 $mm \cdot h^{-1}$ (20 mm of rainfall over 0.5 hour). Therefore, the normalized peak intensity is

$$i_p = \frac{r_p}{i_b} = \frac{240.0}{40.0} = 6.0 \qquad [2.2.4]$$

for the example data.

**2.2.2 The Double Exponential Function for i(t)**

A double exponential function fitted to the normalized intensity pattern is then

$$i(t) = \begin{cases} a\, e^{bt} & 0 \le t \le t_p \\ c\, e^{-dt} & t_p < t \le 1.0 \end{cases} \qquad [2.2.5]$$

which is an equation with four parameters $(a,b,c,d)$ to be determined. If the area under the curve defined by Eq. [2.2.5] from 0.0 to $t_p$ is assumed to be equal to $t_p$, then the area under the curve from $t_p$ to 1.0 is $(1.0 - t_p)$. Using this assumption and the fact that $i(t{=}t_p) = i_p$, Eq. [2.2.5] can be rewritten as

$$i(t) = \begin{cases} i_p\, e^{b(t - t_p)} & 0 \le t \le t_p \\ \\ i_p\, e^{d(t_p - t)} & t_p < t \le 1.0 \end{cases} \qquad [2.2.6]$$

which is now an equation with two parameters $(b,d)$ to be determined.

If $I(t)$ is defined as the integral of $i(t)$, then

$$I(t_p) = \int_0^{t_p} i_p\, e^{b(t - t_p)}\, dt = t_p \qquad [2.2.7]$$

and

$$I(1.0) = \int_{t_p}^{1.0} i_p\, e^{d(t_p - t)}\, dt = 1 - t_p. \qquad [2.2.8]$$

Evaluation of these integrals results in two equations

$$i - e^{bt_p} = \frac{bt_p}{i_p} \qquad [2.2.9]$$

and

$$i - e^{d(1-t_p)} = \frac{d(1-t_p)}{i_p} \qquad [2.2.10]$$

which must be solved for $b$ and $d$. With the above assumptions $i(0)$ is equal to $i(1.0)$ so that $d = b\, t_p/(1-t_p)$. Now, Eq. [2.2.9] need only be solved for $b$ for the entire solution. Newton's method can be used to solve for $b$. If $b$ is restricted to values less than 60, then Newton's method can be used to solve for $b$ with current microcomputers.

The integral $I(t)$ of Eq. [2.2.5] or [2.2.6] can be written as

$$I(t) = \begin{cases} (a/b)\,(e^{bt}-1) & 0 \le t \le t_p \\ \\ (-c/d)\,(e^{d(t_p-t)}-1) & t_p < t \le 1.0 \end{cases} \qquad [2.2.11]$$

where, from above $a = i_p\, e^{-bt_p}$, $c = i_p\, e^{dt_p}$, and $0.0 \le I(t) \le 1.0$. Subdividing the interval [0,1] into $n$ equal subintervals and calling the right endpoint of these subintervals $F_{1,} F_2 ..., F_n$, specific time values can be defined as $T_{1,}\ T_{2,}\ ...,\ T_{n+1}$. These values of $T_{1,}\ T_{2,}\ ....$ are then defined by inverting the $I(t)$ function. Let *Inverse* $I(t)$ be the inverse of $I(t)$ and then

$$\begin{aligned} T_1 &= Inverse\ I(0.0) = 0.0 \\ T_2 &= Inverse\ I(F_1) \\ T_3 &= Inverse\ I(F_2) \\ T_4 &= Inverse\ I(F_3) \\ &\ \ \vdots \\ T_{n+1} &= Inverse\ I(F_n = 1.0) = 1.0 \end{aligned} \qquad [2.2.12]$$

The average normalized intensity over the interval [ $T_i$, $T_{i+1}$] is then calculated as $I_i = (F_{i+1} - F_i)/(T_{i+1} - T_i)$. The result of these calculations is an array of ordered pairs [$T_i$, $I_i$] which are normalized time-intensity values much like columns 4 and 5 in Table 2.2.1. However, because the values of $F_i$ are on a regular subinterval, the time intervals $T_{i+1}$ - $T_i$ vary inversely with $i(t)$. That is, when $i(t)$ is high, then $T_{i+1}$ - $T_i$ is small and when $i(t)$ is low, $T_{i+1}$ - $T_i$ is large.

The data in Table 2.2.1 indicate that the storm depth, *P*, is 20 mm, the storm duration, *D*, is 30 min, the normalized time to peak intensity, $t_p$, is 0.2, and the normalized peak intensity, $i_p$, is 6.0. Thus, for disaggregation purposes, the example storm is represented by four numbers: *P*, *D*, $t_p$, $i_p$. If n subintervals are used, then the disaggregated time intensity data are: $T_{1,}\ I_{1,}\ ...,\ T_{n+1,}\ I_{n+1}$. To restore the original dimensions, multiply each $T_i$ by *D* and each $I_i$ by (*P* 60.0/*D*). Example calculations for the example data from Table 2.2.1 are shown in Table 2.2.2.

Notice that the peak intensity in Table 2.2.2 is 224.7 $mm{\cdot}h^{-1}$ rather than exactly 240.0 $mm{\cdot}h^{-1}$. This is because the intensity is averaged over the interval from 6.0 to 6.53 min and the average intensity is always less than the instantaneous maximum.

Measured storm data for a ten year period at Chickasha, OK, are summarized in Table 2.2.3. Notice the high variability in the data (the standard deviation is about as large as the mean) for all the variables used to describe the storms.

Table 2.2.2 Example calculations for double exponential disaggregation of the storm shown in Table 2.2.1, with n = 10.

| Dimensionless | | Dimensional | |
|---|---|---|---|
| Time | Intensity | Time | Intensity |
| $T_i$ | $I_i$ | ($min$) | ($mm \cdot h^{-1}$) |
| (1) | (2) | (3) | (4) |
| 0.0 | 0.565 | 0.0 | 22.6 |
| 0.177 | 4.33 | 5.31 | 173.3 |
| 0.200 | 5.62 | 6.00 | 224.7 |
| 0.218 | 4.87 | 6.53 | 194.7 |
| 0.238 | 4.12 | 7.15 | 164.7 |
| 0.263 | 3.37 | 7.88 | 134.7 |
| 0.292 | 2.62 | 8.77 | 104.6 |
| 0.331 | 1.86 | 9.92 | 74.4 |
| 0.384 | 1.10 | 11.5 | 43.8 |
| 0.476 | 0.191 | 14.3 | 7.6 |
| 1.00 | 0.0 | 30.0 | 0.0 |

Table 2.2.3. Summary of storm data with storm amounts greater than or equal to the threshold value, $P_o$. Chickasha, OK, Watershed R-5, 1966-1975.

| Threshold | Number | Precipitation | | Duration | | $t_p$ | | $i_p$ | |
|---|---|---|---|---|---|---|---|---|---|
| $P_o$ | of | Mean | SD | Mean | SD | Mean | SD | Mean | SD |
| ($mm$) | Storms | ($mm$) | ($mm$) | ($h$) | ($h$) | | | | |
| 0.0 | 612 | 10.7 | 14.2 | 2.45 | 2.78 | 0.43 | 0.30 | 4.8 | 5.5 |
| 2.54 | 425 | 15.0 | 15.2 | 3.29 | 2.92 | .39 | .32 | 6.1 | 5.9 |
| 6.35 | 278 | 20.8 | 16.0 | 4.01 | 3.21 | .36 | .29 | 6.8 | 5.7 |
| 12.7 | 177 | 27.3 | 16.9 | 4.49 | 3.53 | .34 | .28 | 7.7 | 6.4 |
| 25.4 | 71 | 41.6 | 18.7 | 5.34 | 4.01 | .32 | .28 | 7.8 | 3.4 |

### 2.2.3 Influence of Disaggregation on Computed Runoff

To determine the influence of the proposed disaggregation scheme on computed runoff, a comparison of how well runoff computed using measured rainfall intensity data compare with runoff computed using the rainfall intensity patterns obtained from the disaggregation. The following steps were taken to make the comparison: (a) select observed rainfall and runoff data from several small watersheds at various locations, (b) apply the Green-Ampt infiltration equation to the observed rainfall data and then adjust the Green-Ampt infiltration parameters ($K_s$, $N_s$) until the measured runoff volume is matched by the computed runoff volume, (c) route the overland flow on a single plane and adjust the hydraulic resistance parameter (Chezy C or friction factor) until the computed peak rate of runoff matches the measured peak rate or is as close to the measured peak as is possible, (d) apply the infiltration equation to the intensity pattern from the disaggregation and route the runoff on the plane using the $K_s$, $N_s$, and $C$ values determined in b and c, and (e) compare the runoff volume and peak rates from step d with those obtained from steps b and c.

The selected watersheds are described in Table 2.2.4 and the observed data are summarized in Table 2.2.5. Notice that soils ranged from sandy loam to clay and that cover conditions ranged from near bare soil to complete cover by pasture grass.

Table 2.2.4. Selected storms for small watersheds, watershed characteristics at time of storms.

| Location | Watershed Area (*acres*) | Watershed Area (*ha*) | Storm Date | Land Use & Management |
|---|---|---|---|---|
| Watkinsville, GA<br>Watershed W-1<br>(Location 10)<br>63% Sa, 21% Si, 16% Cl | 19.2 | 7.77 | 7/11/41 | Bench terraces, broadcast cowpeas in rotation with cotton |
| | | | 5/15/42 | Cotton, 2-3" high, soil loose and without vegetative cover |
| | | | 5/26/66 | Terraces removed in 1957. Good, grazed coastal Bermuda grass, complete cover |
| | | | 3/19/70 | Dormant coastal Bermuda grass, just beginning spring growth, excellent cover |
| Riesel, TX<br>Watershed SW-17<br>(Location 42)<br>70% Houston Black clay<br>30% Heiden clay | 2.89 | 1.21 | 3/31/57 | 100% Bermuda grass pasture with burrclover, weeds, dense growth |
| | | | 8/12/66 | 100% Bermuda grass pasture 2-4" high, good cover, not grazed |
| | | | 7/19/68 | 100% Bermuda grass pasture 10" high |
| | | | 3/23/69 | 100% Bermuda grass pasture 6" high |

Source of data: USDA-ARS 1963. Hydrologic data for experimental agricultural watersheds in the United States, 1956-9. USDA Misc. Publication No. 945, US Dept. of Agriculture, Agricultural Research Service, Washington, DC. Also subsequent Misc. Publications of the same title, through 1971.

Table 2.2.4. Selected storms for small watersheds, watershed characteristics at time of storms. (Cont.)

| Location | Watershed Area acres | (ha) | Storm Date | Land Use & Management |
|---|---|---|---|---|
| Coshocton, OH Watershed 109 (Location 26) Muskingum silt loam | 1.61 | 0.65 | 7/7/69 | Cover of 50-75%, 37" corn; 0-25%, 14" weeds, 75% density |
| | | | 2/22/71 | Chopped corn stalks in field |
| Hastings, NE Watershed 3-H (Location 44) 75% of area is Holdrege silt loam & 25% is Holdrege silty clay loam (severely eroded) | 3.77 | 1.53 | 7/3/59 | Sorghum about 6" high and in good condition. Weeds beginning to grow. Last field operation 6/15/59 |
| | | | 5/21/65 | No tillage during spring. Cover is weeds and wheat stubble. |
| Chickasha, OK (Location 69) Renfro, Grant, & Kingfisher silt loam | 23.7 | 9.59 | 4/10/67 | 100% in virgin native grassland. Continuous grazing slightly in excess of optimum |
| | | | 4/12/67 | 100% in virgin native grassland. Continuous grazing slightly in excess of optimum |
| | | | 5/6/69 | 100% rangeland slightly overgrazed; however, range condition class good to excellent |

Source of data: USDA-ARS 1963. Hydrologic data for experimental agricultural watersheds in the United States, 1956-9. USDA Misc. Publication No. 945, US Dept. of Agriculture, Agricultural Research Service, Washington, DC. Also subsequent Misc. Publications of the same title, through 1971.

The data summarized in Table 2.2.5 represent a wide range of storm sizes and patterns (i.e. P varying from 16 to 104 mm, $D$ from 40 min to 1265 min, etc.). Individual storms selected for analysis were chosen to represent a wide range in durations, alternating periods of high and low intensity, and ranges in time to peak intensity, $t_p$, and peak intensity, $i_p$. Thus, the values of $P$, $D$, $t_p$, and $i_p$ in Table 2.2.5 should provide a harsh test of the disaggregation method.

Table 2.2.5 Summary of selected events for five small watersheds, observed data.

| Watershed | Date | $P$ ($mm$) | $D$ ($min$) | $t_p$ | $i_p$ | $Q$ ($mm$) | $Q_p$ ($mm \cdot h^{-1}$) | Antecedent 5-Day $P$ ($mm$) | Antecedent 5-Day $Q$ ($mm$) |
|---|---|---|---|---|---|---|---|---|---|
| Watkinsville, GA | 7/11/41 | 63.5 | 305 | 0.12 | 11.0 | 33.5 | 49.8 | 59.2 | 26.6 |
| W-1 | 5/15/42 | 50.5 | 71 | .12 | 2.3 | 29.0 | 32.0 | 63.0 | 0.3 |
| (Location 10) | 5/26/66 | 88.6 | 633 | .83 | 11.2 | 42.5 | 17.1 | 25.7 | 0.0 |
| | 3/19/70 | 69.1 | 1131 | .42 | 9.7 | 19.9 | 7.2 | 41.9 | 0.1 |
| Riesel, TX | 3/31/57 | 16.3 | 63 | 0.07 | 8.2 | 6.1 | 11.2 | 41.7 | T |
| SW-17 | 8/12/66 | 104.2 | 382 | .32 | 6.1 | 41.8 | 41.0 | 102.1 | 0.0 |
| (Location 42) | 7/19/68 | 39.1 | 40 | .21 | 1.9 | 12.5 | 19.6 | 0.0 | 0.0 |
| | 3/23/69 | 25.1 | 180 | .62 | 7.3 | 19.7 | 20.1 | 8.1 | 0.1 |
| Coshocton, OH | 7/7/69 | 17.3 | 88 | 0.37 | 6.7 | 3.5 | 24.0 | 2.5 | 0.0 |
| W-109 | 2/22/71 | 20.6 | 1265 | .11 | 6.0 | 10.9 | 3.7 | 8.9 | 0.0 |
| (Location 26) | | | | | | | | | |
| Hastings, NE | 7/3/59 | 66.8 | 45 | 0.16 | 2.3 | 59.7 | 163.8 | 59.4 | 27.7 |
| 3-H | 5/21/65 | 85.4 | 98 | .16 | 2.1 | 57.9 | 79.5 | 5.1 | 0.0 |
| (Location 44) | | | | | | | | | |
| Chickasha, OK | 4/10/67 | 29.4 | 160 | 0.06 | 8.2 | 4.6 | 4.2 | 38.9 | 0.3 |
| R-5 | 4/12/67 | 64.1 | 519 | .15 | 7.3 | 20.5 | 22.3 | 68.3 | 5.1 |
| (Location 69) | 5/6/69 | 43.7 | 380 | .76 | 12.2 | 14.5e | 17.9 | 54.4 | 0.5 |

Runoff data computed using the observed rainfall intensity patterns and computed using the approximate rainfall intensity patterns are summarized in Table 2.2.6. Notice the magnitude of the errors are less for runoff volume, $Q$, than for peak rate of runoff, $Q_p$.

An example of observed rainfall intensity data, the rainfall intensity pattern from disaggregation, and the resulting runoff calculations is shown in Figure 2.2.1. Notice that although the disaggregated intensity pattern does not fit the observed intensity pattern, the calculated runoff agrees quite well with measured runoff. This is not always the case, and significant errors can result from the disaggregation approximations (see Table 2.2.6). However, the overall goodness of fit of the runoff computed with the approximate intensity patterns to the runoff computed with the observed intensity patterns was significant (see Figure 2.2.2). As shown in Figure 2.2.2, using the disaggregated intensity patterns as input to the calibrated infiltration-runoff model explained some 90% of the variance in runoff computed using the observed rainfall intensity patterns.

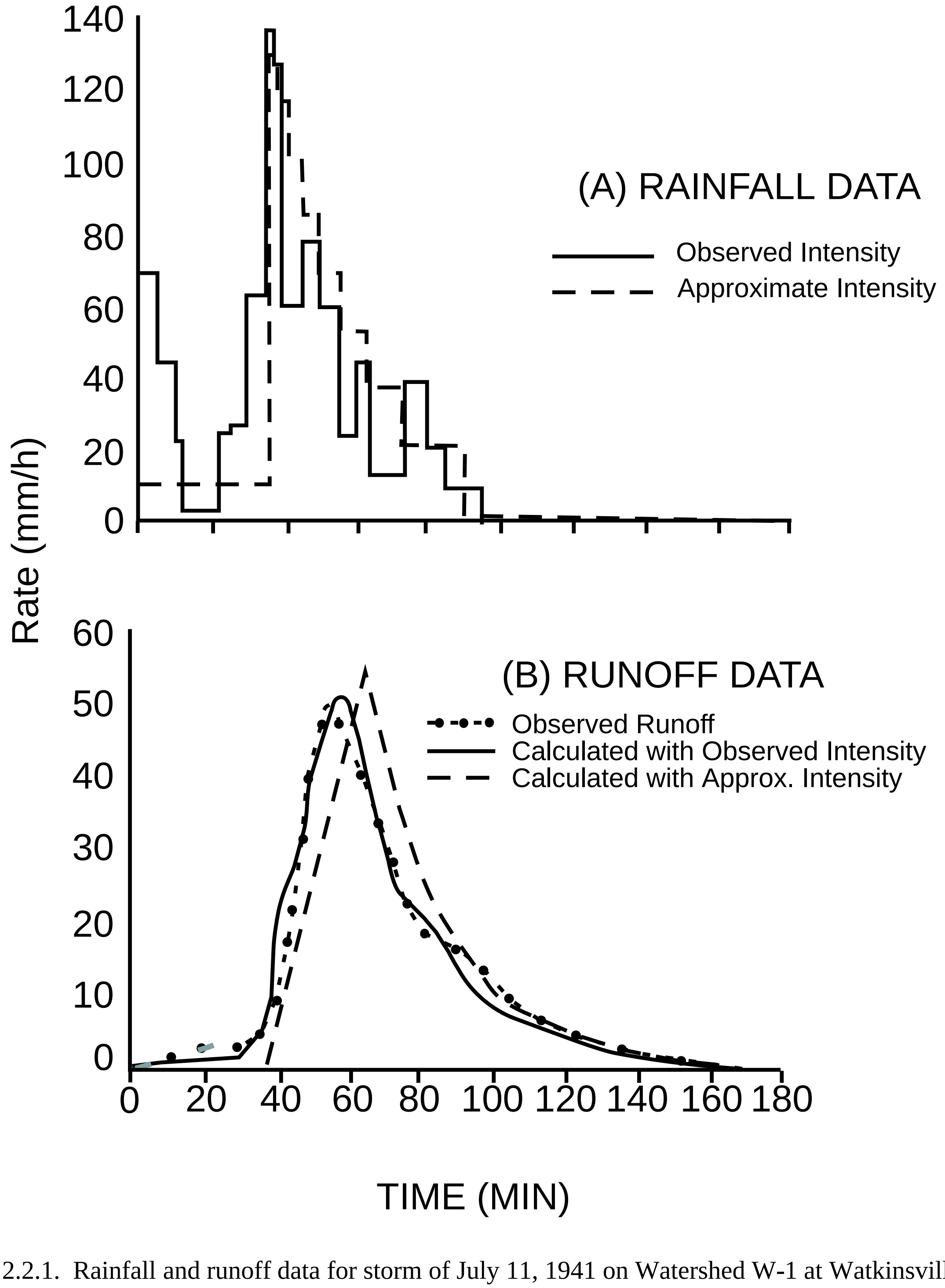


Figure 2.2.1. Rainfall and runoff data for storm of July 11, 1941 on Watershed W-1 at Watkinsville, GA.

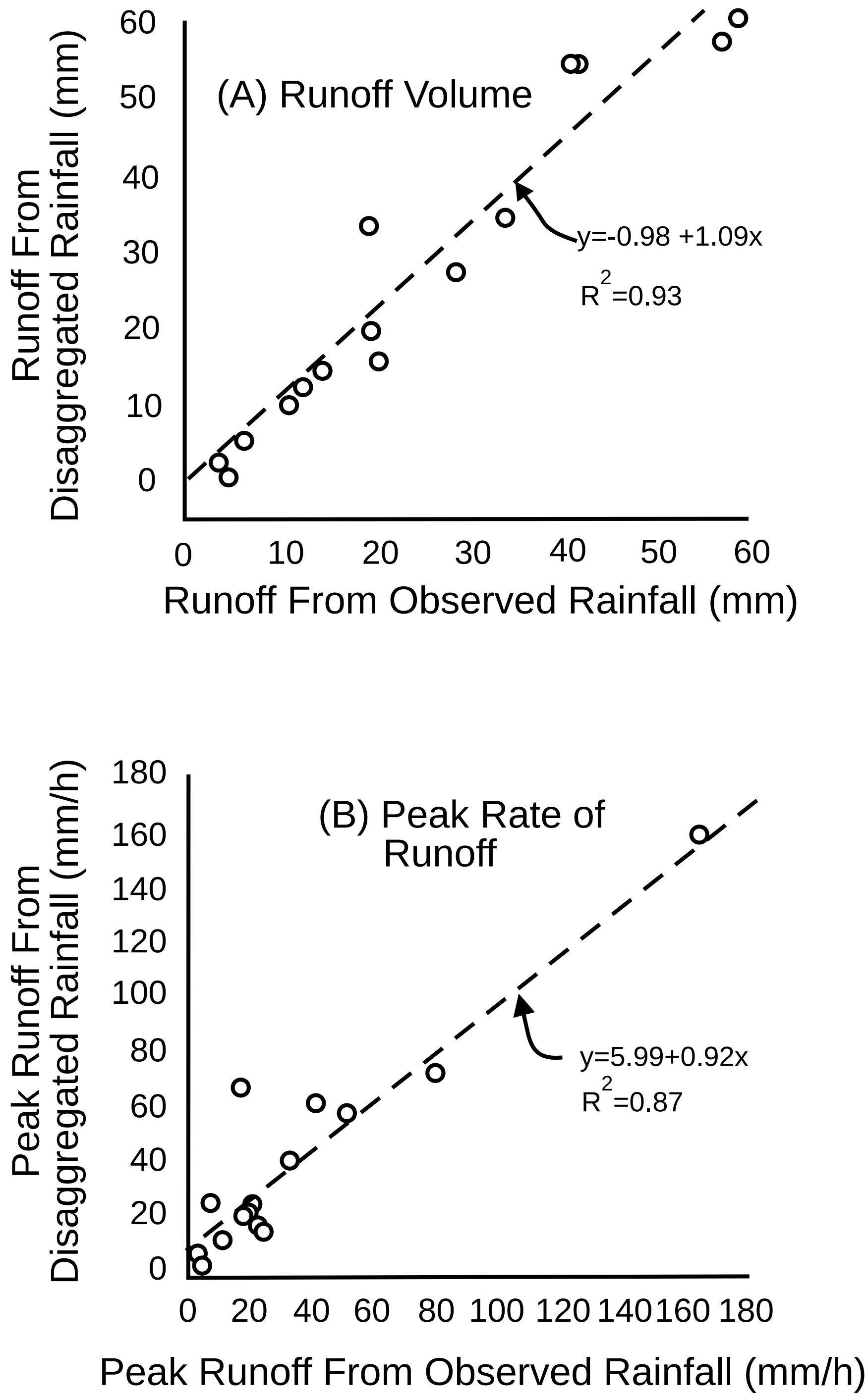


Figure 2.2.2. Relationships between runoff computed using observed and approximated rainfall intensity data.

Table 2.2.6. Summary of observed and computed runoff for selected events on five small watersheds.

| Watershed & Date | Green-Ampt | | Chezy $C$ | Observed Runoff | | Computed Runoff from Measured Rainfall | | Computed Runoff from Disaggregated Rainfall | |
|---|---|---|---|---|---|---|---|---|---|
| | $K_s$ $(mm \cdot h^{-1})$ | $N_s$ $(mm)$ | $(m^{0.5} \cdot s^{-1})$ | $Q$ $(mm)$ | $Q_p$ $(mm \cdot h^{-1})$ | $Q$ $(mm)$ | $Q_p$ $(mm \cdot h^{-1})$ | $Q$ $(mm)$ | $Q_p$ $(mm \cdot h^{-1})$ |
| Watkinsville, GA W-1 L=350, S=.05 | | | | | | | | | |
| 7/11/41 | 7.20 | 22.0 | 5.0 | 33.5 | 49.8 | 34.5 | 50.8 | 34.2 | 55.0 |
| 5/15/42 | 7.20 | 18.7 | 4.7 | 29.0 | 32.0 | 29.0 | 32.2 | 27.3 | 37.4 |
| 5/26/66 | 6.72 | 7.5 | 4.1 | 42.5 | 17.1 | 42.5 | 16.8 | 53.8 | 64.8 |
| 3/19/70 | 4.78 | 7.2 | 3.9 | 19.9 | 7.2 | 19.9 | 7.2 | 33.4 | 22.2 |
| Riesel, TX SW-17 L=119, S=.02 | | | | | | | | | |
| 3/31/57 | 2.57 | 59.2 | 5.5 | 6.1 | 11.2 | 6.1 | 11.2 | 5.2 | 8.8 |
| 8/12/66 | 9.64 | 17.5 | 2.3 | 41.8 | 41.0 | 41.8 | 40.7 | 54.0 | 58.8 |
| 7/19/68 | 16.06 | 21.1 | 3.3 | 12.5 | 19.6 | 12.5 | 19.8 | 12.2 | 18.9 |
| 3/23/69 | 0.65 | 6.6 | 1.9 | 19.7 | 20.1 | 19.7 | 20.3 | 19.8 | 21.2 |
| Coshocton, OH W-109 L= 97, S=.13 | | | | | | | | | |
| 7/7/69 | 8.17 | 29.1 | 8.7 | 3.5 | 24.0 | 3.5 | 24.0 | 2.2 | 11.8 |
| 2/22/71 | 0.40 | 7.1 | 2.1 | 10.9 | 3.7 | 10.9 | 3.7 | 9.9 | 3.7 |
| Hastings, NE 3-H L=163, S=.05 | | | | | | | | | |
| 7/3/59 | 4.16 | 3.8 | 10.0 | 59.7 | 163.8 | 59.7 | 163.8 | 59.7 | 157.1 |
| 5/21/65 | 7.20 | 18.2 | 3.3 | 57.9 | 79.5 | 57.9 | 78.7 | 56.6 | 69.5 |
| Chickasha, OK R-5 L=390, S=.02 | | | | | | | | | |
| 4/10/67 | 11.72 | 42.0 | 10.3 | 4.6 | 4.2 | 4.6 | 4.2 | 0.2 | 0.1 |
| 4/12/67 | 11.72 | 11.9 | 5.8 | 20.5 | 22.3 | 20.5 | 22.2 | 15.7 | 13.8 |
| 5/6/69 | 11.72 | 20.8 | 7.9 | 14.5e | 17.9 | 14.5 | 18.0 | 14.5 | 17.9 |

Note: All watersheds modeled as a single plane and infiltration parameters ($K_s$, $N_s$) selected to match observed runoff volume given the observed rainfall pattern. Chezy C values selected to match the observed peak rates given the observed rainfall.

Possible future improvements in the disaggregation procedure may involve the generation of multiple storm events on the same day. This modification will be undertaken if subsequent analyses of the type described above suggest it is essential to reproduce the probability distributions of runoff and sediment yield.

**2.3 References**


Arnold, J.G. and J.R. Williams. 1989. Stochastic generation of internal storm structure. Trans. ASAE 32(1):161-166.

Arnold, J.G., J.R. Williams, A.D. Nicks and N.D. Sammons. 1990. SWRRB, A Basin Scale Simulation Model for Soil and Water Resources Management. Texas A&M University Press. 236 pp.

Austin, T.A. and B.J. Claborn. 1974. Statistical models of short-duration precipitation events. Proc. of Symposium on Statistical Hydrology, Tucson, AZ, Aug. 31-Sept. 2, 1971. USDA-ARS, Misc. Pub. No. 1275, June 1974, pp. 356-365.

Betson, J.R., J. Bales and H.E. Pratt. 1980. User's guide to TVA-HYSIM. U.S. EPA, EPA-600/7-80, pp. 40-44.

Flanagan, D.C., G.R. Foster and W.C. Moldenhauer. 1987. How storm patterns affect infiltration. Proc. Intrl. Conf. on Infiltration Development and Application, Jan. 6-9, 1987, Honolulu, HI, Univ. of Hawaii, Water Resources Research Center, pp. 444-456.

Foster, G.R. and L.J. Lane (eds.). 1987. User requirements: USDA-Water erosion prediction project (WEPP). NSERL Report No. 1, Sept. 1, 1987. USDA-ARS National Soil Erosion Research Laboratory, West Lafayette, IN. 43 pp.

Franz, D.D. 1974. Hourly rainfall generation for a network. Proc. of Symposium on Statistical Hydrology, Tucson, AZ, Aug. 31-Sept. 2, 1971. USDA-ARS, Misc. Pub. No. 1275, June 1974, pp. 147-153.

Hershenhorn, J. and D.A. Woolhiser. 1987. Disaggregation of daily rainfall. J. of Hydrology 95:299-322.

Nicks, A.D. and J.F. Harp. 1980. Stochastic generation of temperature and solar radiation data. J. Hydrol. 48:1-7.

Nicks, A.D. 1985. Generation of climate data. Proceedings of the Natural Resources Modeling Symposium. USDA-ASA ARS-30. pp. 297-300.

Richardson, C.W. 1981. Stochastic simulation of daily precipitation, temperature and solar radiation. Water Resources Res. 17(1):182-190.

Schaake, J.C., M.J. Ganslaw, J.W. Fothergill and T.E. Harbaugh. 1972. Multivariate rainfall generator for annual, seasonal, monthly, and daily events. Proc. of the International Symposium on Mathematical Modelling Techniques in Water Resources Systems, Vol. 2, pp. 437-460, Environment Canada, Ottawa, Canada.

Skees, P. M. and L.R. Shenton. 1974. Comments on the statistical distribution of rainfall per period under various transformations. Proc. of Symposium on Statistical Hydrology, Tucson, AZ, Aug. 31-Sept. 2, 1971. USDA-ARS, Misc. Pub. No. 1275, June 1974, pp. 172-196.

Srikanthan, R. and T.A. McMahon. 1985. Stochastic generation of rainfall and evaporation data. Australian Water Resources Council Technical Paper No. 84. 301 pp.

Williams, J.R., C.A. Jones and P.T. Dyke. 1984. A modeling approach to determining the relationship between erosion and soil productivity. Trans. ASAE 27(1):129-144.

Williams, J.R., A.D. Nicks and J.G. Arnold. 1985. Simulator for water resources in rural basins. ASCE Hydraulics J. 111(6):970-986.

## 2.4 List of Symbols

| Symbol | Definition | Units | Variable |
|---|---|---|---|
| $A_k$ | accumulated time to peak intensity frequency | - | - |
| $a$ | parameter for the rising limb of the double exponential function | - | a |
| $b$ | parameter for the falling limb of the double exponential function | - | b |
| $c$ | parameter for the rising limb of the double exponential function | - | - |
| $C$ | Chezy hydraulic resistance coefficient | $m^{0.5} \cdot s^{-1}$ | chezyc |
| $d$ | parameter for the falling limb of the double exponential function | - | - |
| $D$ | duration of precipitation event | $h$ | stmdur |
| $D_e$ | Effective precipitation duration | $h$ | dur |
| $D_p$ | time to peak storm intensity | $h$ | timep |
| $D_u$ | upper limit of storm intensity | $h$ | r5u |
| $F_i$ | i$^{th}$ right endpoint of a subinterval on [0,1] | - | - |
| $g$ | skew coefficient of daily precipitation in a month | - | rst(mo,3) |
| $i$ | average rainfall intensity for a time interval | $mm \cdot h^{-1}$ | avrint |
| $i_b$ | average rainfall intensity for a storm | $mm \cdot h^{-1}$ | int |
| $i_p$ | dimensionless ratio of peak to average rainfall intensity | - | ip |
| $i(t)$ | dimensionless rainfall intensity | - | intd1 |
| $I(t)$ | integral of the dimensionless rainfall intensity | - | - |
| $k$ | class interval for time to peak [1,12] | - | - |
| $K_s$ | Green-Ampt equation parameter, hydraulic conductivity | $mm \cdot h^{-1}$ | ks |
| $L$ | length of overland flow plane | $m$ | slplen |
| $n$ | number of equal subintervals on [0,1] | - | - |
| $N$ | total number of storm events | - | - |
| $N_k$ | number of storms in class interval | - | - |
| $N_s$ | Green-Ampt equation parameter, capillary potential | $mm$ | sm |
| $P$ | precipitation amount | $mm$ | rain |
| $P_o$ | threshold precipitation amount | $mm$ | - |
| $P(D \mid D)$ | conditional probability of a dry day, *D*, following a dry day, *D* | - | prw(1,mo) |
| $P(D \mid W)$ | conditional probability of a dry day *D* following, a wet day, *W* | - | prw(2,mo) |
| $P(W \mid D)$ | conditional probability of a wet day, *W*, following a dry day, *D* | - | 1 - prw (1, mo) |
| $P(W \mid W)$ | conditional probability of a wet day, *W*, following a wet day, *W* | - | 1 - prw (2, mo) |
| $Q$ | runoff volume | $mm$ | runoff |
| $Q_p$ | peak rate of runoff | $mm \cdot h^{-1}$ | peakro |
| $RA$ | generated daily solar radiation | $Ly$ | rad |
| $RA_m$ | mean monthly solar radiation | $Ly$ | obsl |

| | | | |
|---|---|---|---|
| $RA_{max}$ | maximum possible solar radiation for a day of the year | $Ly$ | rmx |
| $rl$ | dimensionless parameter in a gamma distribution | - | r1 |
| $r_p$ | storm peak intensity | $mm \cdot h^{-1}$ | rsp |
| $s$ | standard deviation of daily precipitation in a month | $mm$ | rst (mo,2) |
| $S$ | slope of overland flow plane | $m \cdot m^{-1}$ | avgslp |
| $ST_{mn}$ | standard deviation of minimum temperature for a month | $^oC$ | stdtm |
| $ST_{mx}$ | standard deviation of maximum temperature for a month | $^oC$ | stdtx |
| $t$ | dimensionless time | - | - |
| $T_{dp}$ | daily mean dew point temperature | $^oC$ | tdp |
| $T_{dpo}$ | monthly mean dew point temperature | $^oC$ | tdpo |
| $T_i$ | inverse of $I(F_i)$ | - | - |
| $T_{max}$ | generated maximum daily temperature | $^oC$ | tmxg |
| $T_{min}$ | generated minimum daily temperature | $^oC$ | tmxg |
| $T_{mn}$ | mean daily minimum temperature for a given month | $^oC$ | obmn |
| $T_{mx}$ | mean daily maximum temperature for a given month | $^oC$ | obmx |
| $u$ | mean of daily precipitation in a month | $mm$ | rst(1, mo) |
| $U_{ra}$ | standard deviation of daily solar radiation for a month | $Ly$ | stdsl |
| $v$ | standard normal deviate | - | v |
| $x$ | standard normal variate | - | x |
| $X$ | skewed normal random variable representing daily precipitation | - | X |
| $\alpha$ | conditional probability of a wet day following a dry day | - | - |
| $\beta$ | conditional probability of a dry day following a wet day | - | - |